

Probe and Control of the Reservoir Density of States in Single-Electron Devices

M. Möttönen,^{1,2,3,4} K. Y. Tan,^{1,2} K. W. Chan,² F. A. Zwanenburg,² W. H. Lim,²
 C. C. Escott,² J.-M. Pirkkalainen,^{2,3} A. Morello,² C. Yang,⁵ J. A. van Donkelaar,⁵
 A. D. C. Alves,⁵ D. N. Jamieson,⁵ L. C. L. Hollenberg,⁵ and A. S. Dzurak²

¹These authors contributed equally.

²Centre for Quantum Computer Technology, School of Electrical Engineering & Telecommunications,
 University of New South Wales, Sydney NSW 2052, Australia.

³Department of Applied Physics/COMP, Helsinki University of Technology, P.O. Box 5100, FI-02015 TKK, Finland.

⁴Low Temperature Laboratory, Helsinki University of Technology, P.O. Box 3500, FI-02015 TKK, Finland.

⁵Centre for Quantum Computer Technology, School of Physics, University of Melbourne, Melbourne VIC 3010, Australia.

(Dated: June 2, 2018)

We present a systematic study of quasi-one-dimensional density of states (DOS) in electron accumulation layers near a Si–SiO₂ interface. In the experiments we have employed two conceptually different objects to probe DOS, namely, a phosphorus donor and a quantum dot, both operating in the single-electron tunneling regime. We demonstrate how the peaks in DOS can be moved in the transport window independently of the other device properties, and in agreement with the theoretical analysis. This method introduces a fast and convenient way of identifying excited states in these emerging nanostructures.

PACS numbers: 73.21.-b, 61.72.uj, 83.35.-p

The appearance of discrete energy spectra is often regarded as a fundamental property of quantum systems. However, the limit of vanishing energy spacing can be met in many mesoscopic systems at the interface of the quantum and classical regimes meaning that the energy levels can be treated as a continuum. This gives rise to the concept of density of states (DOS), the integral of which over an energy domain yields the number of quantum states in that region. The DOS concept has been successfully applied in explaining transport, absorption and emission, and quantum statistical phenomena in such devices [1]. In particular, DOS is a key element in the low-temperature behavior of metal-oxide-semiconductor field-effect transistors [2] (MOSFETs) which constitute the cornerstone of information processing circuits today. Since device miniaturization has now reached the point where quantum effects of single atoms can dominate the operation characteristics [3, 4, 5, 6], there is an urgent need to understand and distinguish continuum DOS effects from the discrete quantum behavior. In this paper we present a systematic study of the reservoir DOS in two gated MOSFET nanostructures with quantum channels defined by either a quantum dot or the extreme case of a single donor atom.

In a silicon MOSFET a positive gate voltage is applied to induce an electron layer directly below the Si–SiO₂ interface. Hence, the electron dynamics is essentially limited to two dimensions, leading ideally to a constant DOS. In a narrow channel, however, the continuum approximation is only valid in the longest direction, giving rise to quasi-one-dimensional (Q1D) DOS with highly non-uniform characteristics, see Fig. 1(a). Conductance modulations attributed to Q1D density of states were first observed in a parallel configuration of 250

narrow MOSFET channels [7] and later in a single channel [8, 9, 10]. Since the cumulative conductance through all occupied states was measured in these experiments, the studies were limited to rather low electron densities in the channel. The Q1D density of states is also intimately related to ballistic electron transport through quantum point contacts [11, 12], and has been probed in single carbon nanotubes using scanning tunneling microscopy [13, 14].

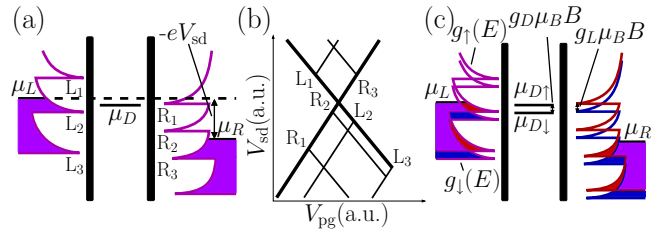


FIG. 1: (Color online) (a) Schematics of single-electron tunneling through a discrete quantum level, μ_D , together with the reservoir Fermi levels, $\mu_{L/R}$, and density of states. (b) Schematic stability diagram showing conductance through the discrete quantum level as a function of the source–drain bias and the plunger gate voltage. The numbered lines of increased conductance arise from the corresponding DOS peaks in panel (a). (c) Zeeman splitting of the reservoir and discrete energy levels in a magnetic field.

In single-electron transport through discrete quantum states [1], the current is directly proportional to the reservoir DOS at a given energy, see Fig. 1. Considerable effort has been directed towards the study of local density of states of a reservoir in the vicinity of an impurity atom in a GaAs quantum well [15, 16, 17]. Here, the local DOS was dominated by disorder due to impurity scat-

tering, resulting in reproducible but irregular features in the conductance which behaved in a complicated way as a function of magnetic field. Thus the term local DOS fluctuations was introduced. In our case, the behavior is less complicated, and hence we do not refer to peaks in DOS as fluctuations.

In gated devices, local DOS effects have also been observed in tunneling through a vertical quantum dot [18], for which a schematic stability diagram is shown in Fig. 1(b). Recently, gated quantum dots have attracted great interest due to their tunability, and lines in the stability diagrams not attributed to excited states have been observed in various structures [19, 20, 21]. In Refs. [20, 21] however, these lines were due to phonon modes, whereas in Ref. [19] they were suggested to arise from reservoir DOS but were not studied thoroughly.

Motivated by the Kane proposal [22] for a quantum computer based on shallow donors in silicon [23], there has been considerable development in electron transport through gated single donors [3, 4, 5, 6]. In these experiments, conductance lines attributed to reservoir DOS have been observed but, again, not studied in detail. Indeed, it has not yet been proven that these features are due to the reservoir DOS. In this paper we present a systematic study of the reservoir DOS in two different nanostructures, namely, in a recently introduced double-gated single-donor transistor [6] (Structure A) and in a novel multi-gated silicon quantum dot [24] (Structure B), shown in Fig. 2. In contrast to previous studies of DOS, the double- and multi-gated designs allow us to map conveniently the reservoir DOS at a wide range of energies and electron densities.

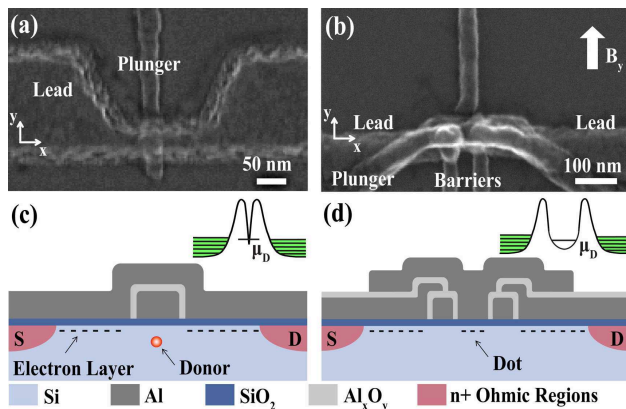


FIG. 2: (Color online) (a) Top view of Structure A and (b) Structure B and a schematic cross section of (c) Structure A and (d) Structure B in the $y = 0$ plane. The insets show schematic potential landscapes along x .

The high-purity [001] silicon substrates for both device structures went through similar fabrication steps to those described in detail in Ref. [6]. In Structure B, however, there are three layers of metallic gates deposited with no implanted donors underneath. The working principle of

both devices is that an accumulation layer of electrons is induced directly below the Si-SiO₂ interface using the lead gate voltage V_{lg} . This layer constitutes the reservoirs for single-electron tunneling through a single donor or a quantum dot, the electrochemical potentials of which can be tuned by the plunger gate voltage V_{pg} . For Structure A, the plunger gate works also as a barrier gate, depleting the reservoirs in the vicinity of the donor. For Structure B, however, we have separate barrier gates which can be used to tune the coupling of the quantum dot to the left and right reservoir independently. The electron densities in the reservoirs can also be controlled independently, but for simplicity, we keep them at the same value here. As the plunger gate voltage is increased, the electrochemical potential of the donor or dot, μ_D , shifts down, eventually entering the source-drain bias window leading to single-electron tunneling through the device, see Fig. 1(a–b).

The sequential tunneling rate is directly proportional to the reservoir density of states, which leads to a peak in the source-drain current if μ_D is aligned with a peak in the density of states. Critically in our devices, we can shift the Fermi levels of the reservoirs with respect to the conduction band minima by changing the lead gate voltage, V_{lg} , which in turn moves the DOS peaks with respect to the transport window. The effect of the lead gate voltage on μ_D can be compensated by the plunger gate [25]. Therefore, if we observe a conductance peak to shift with V_{lg} in the stability diagram, we can identify it to arise from a peak in the reservoir DOS, clearly distinct from features due to excited states in the dot or donor which do not move with V_{lg} . Previously, DOS peaks have been probed by changing the temperature [17] or magnetic field [26], both of which also have an impact on the donor or the dot, and which are many orders of magnitude slower than the method presented here.

The measurements were carried out in ³He-⁴He dilution refrigerators below 100 mK temperatures. The conductance was measured using standard lock-in techniques and the direct current was measured from the same signal after low-pass filtering the modulation arising from the 10–50 μ V lock-in excitation. For Structure B, only the direct current was recorded and the differential conductance was extracted numerically.

Figure 3 shows measured stability diagrams for Structure A [panel (a)] and B [panel (d)]. In Structure A the coupling of the donor to the left reservoir is much weaker than to the right reservoir, and hence only lines with positive slopes corresponding to the left reservoir are visible. This is justified by the sequential tunneling model, in which the current through the device is given by $I = 2e\Gamma_{in}\Gamma_{out}/(2\Gamma_{in} + \Gamma_{out})$, where $\Gamma_{in/out}$ is the in/out-tunneling rate. Thus the current is determined by the small rate, independent of whether it corresponds to in- or out-tunneling. The tunneling rates in Structure B can be tuned to be symmetric, but considerable asymmetry persists in the working point of Fig. 3.

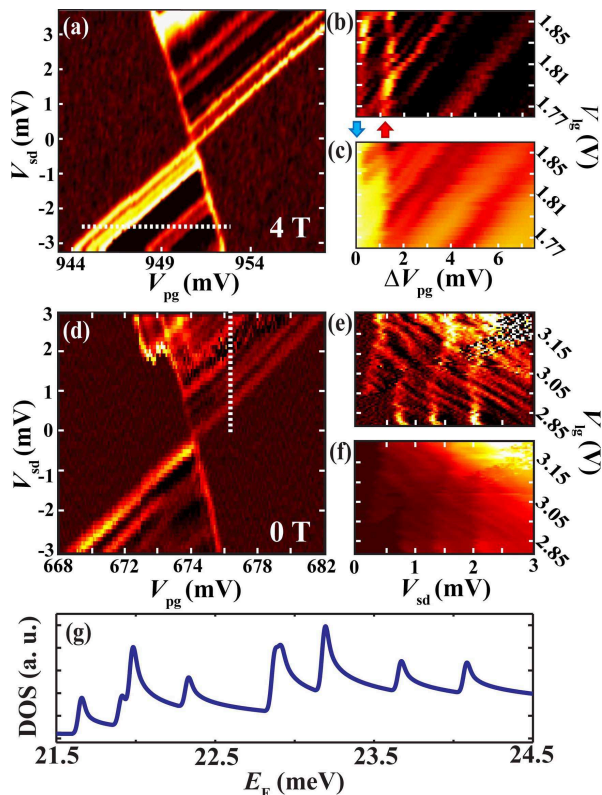


FIG. 3: (Color online) Conductance of (a) Structure A with $V_{\text{lg}} = 1.87$ V and $B_{\parallel} = 4$ T, and (d) Structure B with $V_{\text{lg}} = 3.00$ V, $V_{\text{lb}} = 0.52$ V, $V_{\text{rb}} = 0.68$ V, and $B_{\parallel} = 0$ T as a function of the source–drain bias and the plunger gate voltage. The dashed line in panel (a) represents the trace shown in panels (b) and (c) for $V_{\text{sd}} = -2.5$ mV as a function of the lead gate voltage for differential conductance and direct current, respectively. Panels (e) and (f) correspond to the dashed trace shown in panel (d) for $\Delta V_{\text{pg}} = 2.1$ mV from the transport window at $V_{\text{sd}} = 0$. The capacitive coupling of the lead gate to the donor or the dot has been compensated by the plunger gate in the traces. Panel (g) shows the theoretical prediction for DOS corresponding to panels (b,c). Here, Eq. (1) has been convolved with the Gaussian $\exp\{-E_F^2/[2(500 \mu\text{eV})^2]\}$ to account for broadening due to experimental nonidealities.

The stability diagrams shown in Fig. 3(a,d) do not provide enough information to distinguish whether a specific conductance feature is due to the reservoir DOS or an internal excited state. However, the lead-gate-compensated traces shown in Fig. 3(b,c,e,f) reveal the origin of the conductance peaks. Most of the peaks move with the lead gate voltage, and hence correspond to the reservoir DOS. However, Fig. 3(b,c) shows a feature 0.4 meV above the ground state for all V_{lg} . As justified by measurements carried out in various magnetic fields (see Fig. 4), this line corresponds to the spin excited state of the neutral donor orbital ground state. Similarly, the vertical lines in Fig. 3(e,f) are attributed to excited states of the dot.

For Structure A, the slope of the DOS lines yields the

response of the Fermi level E_F to the lead gate voltage to be $\Delta(E_F - E_c)/\Delta V_{\text{lg}} = (11.3 \pm 1.5)$ meV/V, where E_c is the conduction band minimum. We have modeled this response using technology computer aided design [27] taking into account the three-dimensional geometry of the system. By matching the measured and modeled traces, we obtain an estimate of the absolute value of the Fermi level to be $E_F - E_c = (25 \pm 5)$ meV.

The average energy spacing between the DOS peaks is obtained from Fig. 3 to be (0.33 ± 0.03) meV for Structures A and B. We model this by calculating the single-particle energy spectrum for a triangular well $V_z(z) = eF|z|/\Theta(-z)$ in the z direction (Θ is the Heaviside step function), an infinite $W = 70$ nm box potential in the y direction, and a semi-infinite box potential in the x direction. Here, F is the electric field in the vicinity of the Si–SiO₂ interface due to the lead gate. The one-dimensional DOS in the x direction, for which the continuum approximation is valid, is given by $D_{1d}(E) = \sqrt{2m_x}/(\pi\hbar\sqrt{E})$, where m_x is the effective mass of the electron in the x direction. Thus we obtain for the total density of states

$$D(E) = \frac{\sqrt{2}}{\pi\hbar} \sum_{n_y, n_z, n_v} \frac{\sqrt{m_{x,n_v}} \Theta[E - E_{y,z}(n_y, n_z, n_v)]}{\sqrt{E - E_{y,z}(n_y, n_z, n_v)}}, \quad (1)$$

where n_y , n_z , and n_v are the indices for the energy levels in the y , z , and valley degrees of freedom, respectively. The six-fold valley degeneracy of bulk silicon is lifted due to different effective masses $m_t = 0.190 \times m_0$ and $m_l = 0.916 \times m_0$ for the transverse and longitudinal directions, respectively [2]. Here, m_0 is the electron rest mass. Thus the effective mass in the x direction depends on the valley degree of freedom. According to Eq. (1), a peak in DOS is observed at energies matching the single-particle energy levels in the two-dimensional yz potential, i.e., for $E = E_{y,z}(n_y, n_z, n_v)$.

The peak spacing resulting from the confinement in the y direction is given by $\pi^2\hbar^2(n_y + 1/2)/(m_y W^2)$. This yields the minimum peak spacing of 1.2 meV for the transverse and 0.25 meV for the longitudinal effective masses. Each excited state in the valley and z degree of freedom superimposes an additional series of peaks, and hence the resulting DOS structure can be rather complicated. Figure 3(g) shows the DOS in the vicinity of the Fermi level obtained above for Structure A. The electric field of is chosen to be $F = 2$ MV/m to match the peak separation observed in the experiments. This field is approximately an order of magnitude lower than expected due to the crude model used to calculate the peak spacing. This simple model does not include the true details of the trapping potential including disorder or the electric field induced by the accumulation layer, which calls for deeper theoretical analysis. Furthermore, we have not included the possible splitting of all valley degeneracies which would further reduce the average peak spacing and consequently, increase the required electric field.

Figure 1(c) shows a schematic diagram of how the DOS peaks behave in magnetic field $\mathbf{B} = B\hat{y}$. The Zeeman effect shifts the kinetic energy at the Fermi level ($E_F - E_c$) for the spin-down electrons up by $g_L\mu_B B/2$, and vice versa for spin-up electrons. Here, g_L is the electron g factor in the reservoirs and $\mu_B = e\hbar/(2m_0)$. Thus the effect of this term is to shift and split the DOS peaks. However, if the electron g factor for the donor or dot, g_D , is almost the same as g_L , this compensates for the splitting and results only in a downwards shift of the DOS peaks by $g_L\mu_B B/2$ with respect to the transport window. In our case, the DOS peaks simply shift and do not split in magnetic field, as demonstrated in Fig. 4, which implies $g_D \approx g_L \approx 2$ consistent with previous measurements [28]. In contrast, Zeeman splitting of DOS peaks has been observed in tunneling through a Si shallow donor in a GaAs/AlAs/GaAs junction [26].

Figure 4(d) shows the energy shift δE of the conductance peaks with respect to the transport window as a function of magnetic field. We observe that within the estimated error, the shift of the DOS peaks and the spin excited state is in agreement with $\delta E = \mu_B B$ and $\delta E = 2\mu_B B$, respectively. Thus our observations can be explained by the Zeeman effect alone.

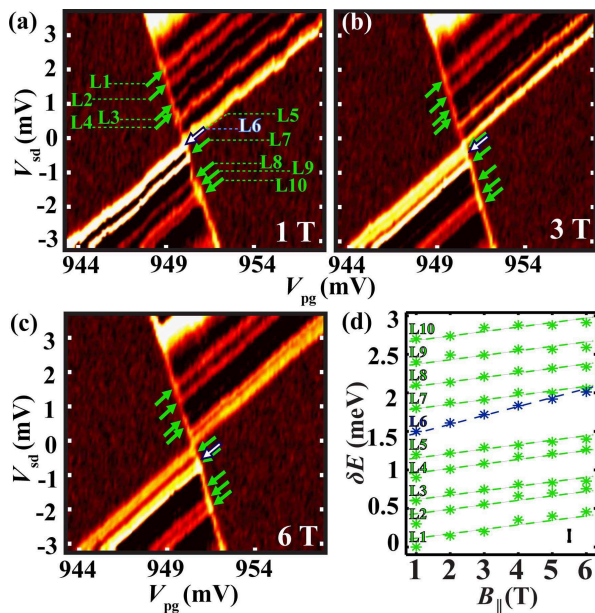


FIG. 4: (Color online) (a–c) Stability diagrams of Structure A in magnetic fields ranging from 1 to 6 T. The spin excited state [L6 in panel (a)] is marked with a white and blue arrow, and the DOS lines are labeled with green arrows. (d) Shift of the conductance lines in magnetic field. Data for each line is offset in energy for clarity. The dashed lines show a slope $2\mu_B$ for L6 and μ_B for the other data.

In conclusion, we have reported the first studies of reservoir DOS in nanostructures through gate control of the reservoir electron density. Magnetic field spectroscopy of the DOS peaks revealed behavior consistent

with energy shifts due to the Zeeman effect alone. Both the single donor and the quantum dot devices studied exhibited similar conductance patterns arising from the reservoir DOS. Our findings not only confirm the interpretation that additional conductance lines observed previously in transport through single donors are due to reservoir states [3, 5, 6], but also demonstrate that these states can be controlled and studied in a quantitative manner.

The authors thank F. Hudson, D. Barber, and R. P. Starrett for technical support, E. Gauja, A. Cimmino, and R. Szymanski for assistance in nanofabrication, and M. Eriksson, J. P. Pekola, and V. Pietilä for insightful discussions. M. M. and J.-M. P. acknowledge Academy of Finland, Emil Aaltonen Foundation, and Finnish Cultural Foundation for financial support. This work is supported by the Australian Research Council, the Australian Government, the U.S. National Security Agency (NSA), and the U.S. Army Research Office (ARO) (under Contract No. W911NF-08-1-0527).

-
- [1] D. V. Averin and K. K. Likharev, In *Mesoscopic Phenomena in Solids*, Edited by B. L. Altshuler, P. A. Lee, and R. A. Webb (Elsevier, Amsterdam, 1991), pp. 173.
 - [2] T. Ando *et al.*, *Rev. Mod. Phys.* **54**, 437 (1982).
 - [3] H. Sellier *et al.*, *Phys. Rev. Lett.* **97**, 206805 (2006).
 - [4] L. E. Calvet *et al.*, *Phys. Rev. Lett.* **98**, 096805 (2007).
 - [5] G. P. Lansbergen *et al.*, *Nature Phys.* **4**, 656 (2008).
 - [6] K. Y. Tan *et al.*, arXiv:0905.4358 (unpublished, 2009).
 - [7] A. C. Warren *et al.*, *Phys. Rev. Lett.* **56**, 1858 (1986).
 - [8] K. Morimoto *et al.*, *Jpn. J. Appl. Phys.* **35**, 853 (1995).
 - [9] H. Matsuoka *et al.*, *J. Appl. Phys.* **76**, 5561 (1994).
 - [10] K. Takeuchi and R. Newbury, *Phys. Rev. B* **43**, 7324 (1990).
 - [11] B. J. van Wees *et al.*, *Phys. Rev. Lett.* **60**, 848 (1988).
 - [12] D. A. Wharam *et al.*, *J. Phys. C* **21**, L209 (1988).
 - [13] J. W. G. Wildöer *et al.*, *Nature* **391**, 59 (1998).
 - [14] L. C. Venema *et al.*, *Phys. Rev. B* **62**, 5238 (2000).
 - [15] J. P. Holder *et al.*, *Phys. Rev. Lett.* **84**, 1563 (1999).
 - [16] T. Schmidt *et al.*, *Phys. Rev. Lett.* **78**, 1540 (1997).
 - [17] T. Schmidt *et al.*, *Europhys. Lett.* **36**, 61 (1996).
 - [18] L. P. Kouwenhoven *et al.*, *Science* **278**, 1788 (1997).
 - [19] M. T. Björk *et al.*, *Nano Lett.* **4**, 1621 (2004).
 - [20] F. A. Zwanenburg *et al.*, *Nano Lett.* **9**, 1071 (2009).
 - [21] R. Leturcq *et al.*, *Nature Phys.* **5**, 327 (2009).
 - [22] B. Kane, *Nature* **393**, 133 (1998).
 - [23] R. Vrijen *et al.*, *Phys. Rev. A* **62**, 012306 (2000).
 - [24] W. H. Lim *et al.*, arXiv:0910.0576 (2009).
 - [25] An increment in the lead gate voltage also results in a slight increase of the transparency of the tunnel barriers. In Structure B, this can be compensated by decreasing the voltage on the barrier gates.
 - [26] B. Jouault *et al.*, *Phys. Rev. B* **79**, 041307(R) (2009).
 - [27] Technology Computer Aided Design modeling package, Integrated Systems Engineering AG, Zurich.
 - [28] L. H. Willems van Beveren *et al.*, *Appl. Phys. Lett.* **93**, 072102 (2008).